8 Visualizing Immune Responses in Fungal Infections: Established and Novel Methods

Mike Hasenberg[1], Sven Krappmann[2], Matthias Gunzer[1]

CONTENTS

I. Introduction

A large variety of fungal species belong to the normal flora of human skin and mucosal tissues and can colonize hosts throughout life. Furthermore, due to environmental interaction, e.g., breathing of ordinary air, people come into contact with huge numbers of fungal elements (Latge 1999). Interestingly, under normal conditions neither colonization nor environmental exposure cause recognizable health problems (Latge 1999). This is due to permanent mutual control by other members of the microbiome (Peleg et al. 2010) and also by the effective barrier function and immune system of the host (Hasenberg et al. 2011a, 2013). However, when either the barrier is broken or the immune system loses its grip, environmental or commensal fungi can infect the host, a condition that is one of the most dangerous threats to human health (Romani 2011; Denning and Hope 2010).

In the clinical daily routine, one of the key problems of mycological infections is the difficulty in clearly and rapidly identifying a fungal infection and differentiating it from other microbial infections. In the face of these problems, a typical therapeutic regime with risk patients suffering from fever of unknown origin is prophylactic treatment with antibiotics, followed by antimycotics if the fever has not vanished after 3–7 days (Freifeld et al. 2011).

Thus, obviously, the lack of a definitive and specific diagnosis can lead to inadequate therapy that may compromise the patient's health without addressing the real problem. Reasons for this therapeutic failure are the poor accessibility of adequate patient samples, imprecise detection tools, or the lack of information on the precise localization and extent of fungal growth.

Whole-body imaging approaches have the potential to address many of these problems at once: techniques like **X-ray chest scans** including **computed tomography (CT)** are able to detect fungal masses in lungs. However, these images are often difficult to interpret such that a fungal mass cannot easily be differentiated from "shadows" caused by other lung afflictions (Muller et al. 2002). A much better soft-tissue contrast, allowing a more precise estimation of fungal masses, can be obtained by **magnetic**

[1]Institute for Experimental Immunology and Imaging, University Duisburg-Essen, University Hospital, Hufelandstrasse 55, 45147 Essen, Germany; e-mail: Matthias.gunzer@uni-due.de
[2]Microbiology Institute – Clinical Microbiology, Immunology and Hygiene, University Hospital of Erlangen and Friedrich-Alexander-Universität Erlangen-Nürnberg, Wasserturmstrasse 3/5, 91054 Erlangen, Germany

Human Fungal Pathogens, 2nd Edition
The Mycota XII
O. Kurzai (Ed.)

resonance imaging (MRI), but still without a definitive identification of a fungal species. Specificity for an inflammatory process can be brought in to a certain extent with **positron emission tomography (PET)** by using metabolic tracers such as [^{18}F]fluorodeoxy-D-glucose (FDG) (Seshadri et al. 2007), but signals generated in this imaging approach can also be obscured or modulated by completely unrelated inflammatory processes such as cancer (Shrikanthan et al. 2005). Thus, more specific tracers such as siderophores, which are used by fungi to trap iron from the host, can be functionalized for **PET** or **PET/MRI** and provide more specific signals, at least in animal models (Petrik et al. 2012). Molecular imaging approaches also have the opportunity to detect "reactivity" or "shadow" anywhere in the body, even at sites normally not sampled for conventional analysis. However, today no available technology, not even FDG-PET imaging, is able to specifically detect the pathogen or the immune response against it in the clinical routine, despite the strong need for such a diagnostic tool.

In addition to diagnostic imaging in clinical applications, another important field of work is experimental imaging. Of course, any clinical application has been developed from preclinical studies in vitro or in suitable animal models. However, experimental imaging also aims at elucidating the basic cell-biological mechanisms behind the obtained data that help to explain the course of the disease or the response of the host towards the fungal attack. Experimental imaging aims to develop techniques that look closely at the immune response of a host, either alone or in combination with imaging of the fungus. Specifically, **complex light** and **confocal microscopy** approaches have allowed an understanding of the dynamics underlying phagocytic responses towards fungal elements in vitro (Behnsen et al. 2007a; Bruns et al. 2010). **Flow cytometry**, in contrast, is able to very rapidly image many cells/pathogen in a short period of time; however, with little resolution. Nevertheless this technology is extremely powerful for answering certain questions on fungal biology. A recent addition to the armament of fungal imagers is **intravital 2-photon microscopy**, which allows observation of immune cells while they are phagocytosing fungal elements or producing neutrophil extracellular traps (NETs). This is a powerful immunological weapon against microbial spreading in intact tissue (Bruns et al. 2010) or in vivo. New developments in the field of light microscopy have brought about very remarkable increases in resolution, such that today light microscopy can resolve structures down to 20–30 nm in size. The key developments here are **stimulated emission depletion (STED)**, **structured illumination (SIM)** and **localization microscopy (STORM/PALM)** (Coltharp and Xiao 2012). To obtain the highest possible resolution, **scanning electron microscopy (SEM)** of surface structures (Behnsen et al. 2007a; Hasenberg et al. 2013) or **transmission electron microscopy (TEM)** of fungal elements internalized by phagocytes has been applied (Ibrahim-Granet et al. 2003). Finally, there is a specific very powerful whole-body imaging approach that so far has only been used in experimental systems, namely **luminescence imaging** (Donat et al. 2012).

Generally, any imaging approach has to be validated for its sensitivity, specificity, and cost. An important issue is, of course, if the question being asked by the clinician or researcher can be answered by the chosen imaging approach. In order to help potential users to decide on a successful imaging strategy for their relevant projects, we have summarized the imaging modalities mentioned above. We have sorted them into the categories of clinical and experimental imaging. Each method is introduced by a brief technical description, followed by specific examples of their use, and concluding with a discussion of the sensitivity, specificity, and cost as well as suitability for a given question. The overall aim of this list is to provide interested users with a rational basis for the choice of a suitable imaging approach. Based on our own experimental experience, most samples for fungal imaging center around the mold *Aspergillus fumigatus*. But of course, all discussed systems can in principle also be used for other fungal species and, where appropriate, we will also mention some examples of these.

II. Experimental Scientific Imaging

We start our excursion with modern imaging systems that are employed in scientific laboratories all over the world to visualize cellular processes in (fungal) infections. The overall goal of these techniques is the generation of imaging data that build the basis for understanding the complex interactions between host immune cells and fungal pathogens under diverse infection conditions. For the development of therapeutic strategies it is of high importance to understand which immune cell types are involved in the antimicrobial fight and with which kinetics. To optimize antifungal treatments clinicians need to know which organs are colonized, at which time point in the course of an infection, and which treatments might display promising effects against the infectious threat. All these parameters can be investigated by the huge variety of experimental in vitro and in vivo imaging approaches.

A. (Time-Lapse) Brightfield/Widefield Microscopy

Due to the inherent complexity of the immune response against fungal infections, researchers initially tend to keep their experiments as simple as possible before more complicated systems are explored. A very common way is to reduce the environmental conditions to the level of single cells or at least to explanted tissues, resulting in focused questions. These entities can subsequently be the focus of a variety of different imaging techniques, starting with a basic light microscope.

The major component of a brightfield microscope is a light source that emits transmission light, which passes the microscopic sample. The diffracted light is finally gathered by an objective, typically positioned opposite the light source. The objective generates the magnified picture of the observed sample, which is then further magnified by the eyepiece. **Combined magnifications of objective and eyepiece in commercial systems reach 40× to 1,000×, with a theoretical maximum resolution of ~200 nm, based on the physics of diffraction** (Hell 2007) (see section on electron microscopy). **The obtained picture has a bright background (hence the name) from the transmission light and the structures of the specimen appear darker due to light absorption.** Because the transmission light fully illuminates the specimen over a wide angle (in contrast to a spot illumination), this technique is **also called widefield microscopy**.

Around 1730, the Italian botanist Pietro Antonio Micheli used such a microscope to catalog molds (Michelio 1729). He was the first to illustrate the fungal genus *Aspergillus* and, more than 100 years later in 1863, the physician Georg W. Fresenius introduced *A. fumigatus* as a new species able to cause severe lung infections (Schmidt 1998). His work was also based on transmission microscopy studies of infected human lung samples.

Although this visualization technique is very old it is still used heavily in modern experimental setups, but now extended by a number of crucial inventions. One central progress was the enhancement of contrast by various optical phenomena such as cross-polarized light, dark field, phase contrast, and differential interference contrast (DIC). Together with very light-sensitive detectors (digital complementary metal–oxide–semiconductor; CMOS) or CCD (charge-coupled device) cameras and objectives with a high numerical aperture, the quality of micrographs has significantly increased over time. Current widefield microscope systems all reach the theoretical resolution barrier of 200 nm and are therefore well suited to visualize cellular behavior and even subcellular processes. The application range of widefield systems was further enlarged when these microscopes were equipped for the detection of fluorescence signals. **By employing widefield fluorescent illumination of pre-labeled biological samples it is possible to specifically detect different cell types, cellular compartments, or metabolic products/states inside of cells.** Like other fluorescence-based methods, the specificity is realized by the use of fluorochrome-coupled monoclonal antibodies, separate pre-labeling of different cells with intracellular fluorescent dyes, or by a change in the fluorescent properties of chemical compounds

during intra- or extracellular reactions (Hasenberg et al. 2011b). A very prominent example is the detection of intracellular calcium ions. Ca^{2+} is a major regulator of central signaling pathways during cell activation, including cellular movement. In order to detect these activation signals, living cells can be loaded with calcium chelating agents such as Fura-2, a polyamino carboxylic acid. This fluorescent dye has excitation maxima at 340 and 380 nm and the ratio of its emissions at these wavelengths directly allows the calculation of the free calcium ion concentration inside a cell (Waibler et al. 2008).

Ca^{2+} imaging can only be done in living cells and requires the observation of cells over a period of time with repetitive imaging. Other dynamic processes like phagocytosis can also only be thoroughly studied if live cell imaging is employed (Behnsen et al. 2007a; Sasse et al. 2013). This so-called **time-lapse widefield microscopy** requires appropriate conditions for the isolated cells and fungal elements under investigation. Modern systems are therefore equipped with fully automated climate chambers that allow the regulation of important vital parameters such as temperature, humidity, and CO_2 concentration. As soon as these key settings are well controlled, cellular behavior can be analyzed under conditions that mimic the natural environment regarding these parameters. Upgraded to this level, widefield microscopes can efficiently be used to answer a variety of questions in the field of fungal biology. They can bring light into unknown processes of fungal life cycles and growth, such as the formation of the Spitzenkörper in growing hyphae (Steinberg 2007), and they are well suited to study immune responses towards fungal morphotypes such as phagocytic events and cellular contact formation under in vitro conditions (Behnsen et al. 2007b; Sasse et al. 2013).

On the other hand, widefield microscopy has clear limitations. As soon as a biological sample is composed of more than one cell layer, the ensuing immense light diffraction negatively influences the system's resolution. In the case of fluorescence imaging, light coming from out-of-focus areas of the sample blurs the image and can even make the generation of useful images impossible. **Therefore, a golden rule for obtaining appropriate image material from transmission light microscopy is to keep the samples as thin as possible.** However, if the experimental question does not allow the use of extremely thin samples or the goal is to maintain multicellular layers for physiological reasons, a powerful alternative approach is confocal laser scanning microscopy (CLSM).

B. Confocal Laser Scanning Microscopy

CLSM is a specific kind of fluorescence light microscopy. The basic idea behind this technique is the illumination of the microscopic specimen in a very narrow spatial volume (x, y, and z dimensions) per time point by using a point source of light rather than a widefield illumination. Typically, this point source is a laser of suitable color. A full picture of the sample is then generated by a scanning process in which the exciting light beam is driven line by line and plane by plane over the whole sample volume, resulting in an optical sectioning. As laser light is a very bright and thin beam this is an optimal light source for this application. However, due to the fact that the sample is not illuminated in its entirety at once, imaging with the eye or a camera is not possible. Instead, the light emitted from a given spot of laser-activated fluorochromes is gathered in real-time by sensitive detectors (typically photomultiplier tubes, PMTs) during the acquisition procedure to generate one pixel of a final image. Here, the use of several independent PMTs and suitable filters also allows the generation of multicolor images. **Taking the *x*, *y*, and *z* coordinates together with the emitted light intensities at each illuminated position, the operation software of these microscopes is able to calculate a final three-dimensional (3D) fluorescence picture of the entire sample.**

To minimize diffraction effects, which negatively influence the resolution of light microscopes in thicker samples, CLSMs are equipped with another decisive feature. A so-called **pinhole** in the light path of the emission light eliminates all light that results from the excitation of fluorochromes in out-of-focus areas in the z-direction. Therefore, these fluorescence

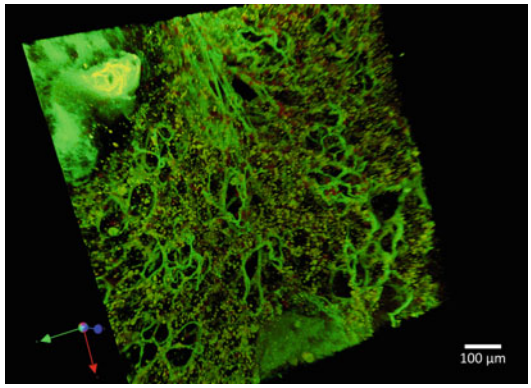

Fig. 8.1. CLSM 3D reconstruction of an *A. fumigatus*-infected lung. This picture has been taken from an infected and subsequently explanted murine lung by use of confocal laser scanning microscopy (CLSM). A 3D rendering was done based on the microscopic sample sections. The organ-specific structures such as alveoli were detected by their autofluorescence signal. The *small red clouds* are so-called neutrophil extracellular traps (NETs), which are composed of extracellular DNA fibers and were released during the neutrophilic immune reaction towards the fungal pathogen. NETs were stained with a DNA-specific dye

signals cannot contribute to the digital calculation of the micrograph at a given position in *z* and as a result the final picture displays much less background noise and can provide a sharp section through a thick sample.

Although this technique does not provide a gain in resolution, the resulting images are usually of a much better quality than comparable widefield fluorescence data from the same sample because they **almost completely lack out-of-focus haze**. In addition, by generating images at different positions in *z*, a CLSM is able to generate series of image planes that result in a real 3D picture of the observed sample (Fig. 8.1). This 3D information is absolutely necessary for all analyses in which the definite spatial localization of certain structures is of importance. With respect to the analysis of the phagocytic uptake of *A. fumigatus* spores by immune cells for example, it is essential to assess from all dimensions around a particular phagocyte whether associated fungal particles have really been ingested or are only attached to the surface of the cell (Mech et al. 2011).

In order to provide a certain flexibility regarding the parallel detection of different fluorescence colors, common CLSM systems are equipped with several lasers and a combination of adjustable excitation and emission filter sets. Very recent machines have been released that use white lasers as light source and can very quickly and precisely tune acousto-optical beam splitters and filters on both the excitation as well as emission side. These systems allow the use of almost all fluorophores that possess a spectral excitation/emission peak in the visible light spectrum.

One disadvantage of note is the speed of image acquisition in a CLSM. As every single two-dimensional (2D) picture is based on the scanning process of the whole specimen in one plane, it takes a certain time until the required digital information for one image is obtained (in contrast to a widefield system in which the picture is recorded by the camera as soon as the specimen is illuminated by the transmission light). Although it is possible to analyze cellular behavior using CLSM (Gunzer et al. 2004), fast moving cells sometimes generate problems when their tracks are the question of the analysis. These problems become even bigger as soon as the cellular movements are analyzed in four dimensions (3D over time). However, novel developments such as resonant scanners and extremely fast and sensitive detectors have helped to partly overcome these problems. Today, the efficiency of light generation from the sample, rather than the slow detection speed of the CLSM, is the key factor limiting the recording speed of a given system.

C. Electron Microscopy

In 1873, Ernst Abbé published a landmark equation that easily correlates the wave nature of light or electrons and the lens properties, thereby calculating the resolving power of a given optical system.

$d = 0.61 \frac{\lambda}{n \cdot \sin a}$	d	Resolution
	λ	Wavelength of the light source
	n	Refractive index of the medium
	α	Aperture angle of the objective

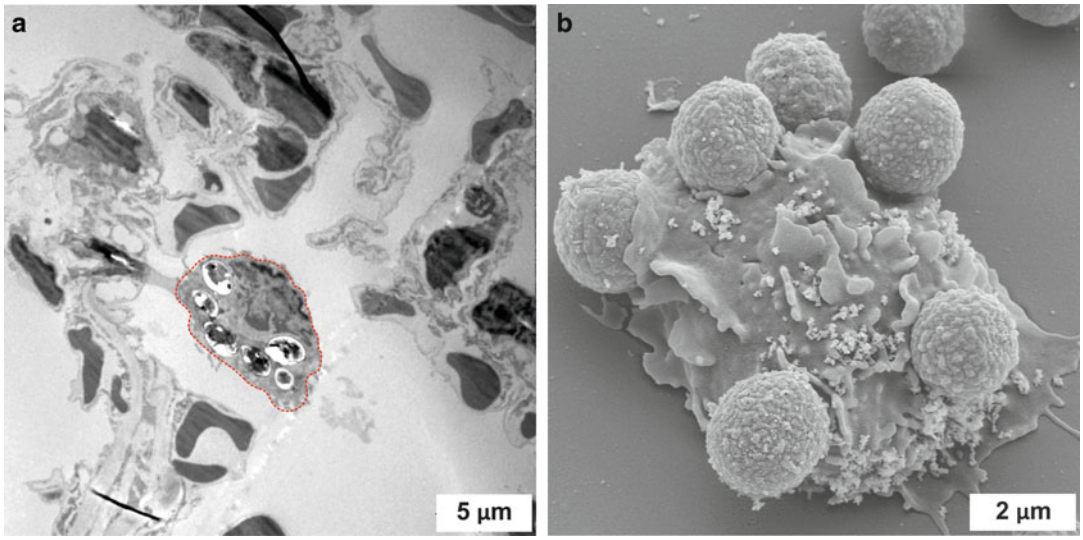

Fig. 8.2. Different appearance of TEM and SEM images. (**a**) Transmission electron microscopy (TEM) image of the situation in an *A. fumigatus*-infected mouse lung. An alveolar macrophage (outlined in *red*) scans the alveolar lumen and has already taken up six fungal spores. (**b**) The scanning electron micrograph (SEM) visualizes the in vitro co-incubation of isolated murine neutrophils and spores of the mold *A. fumigatus* after 4 h. It is nicely observable that the immune cell has started to internalize some of the attached fungal particles. *Scale bars* are depicted in *white*. The pictures were taken in collaboration with Prof. Manfred Rohde at the Helmholtz Center for Infectious Diseases in Braunschweig, Germany

The value d defines the smallest distance between two objects such that they can still be detectable as two separate entities. Thus, the smaller the value for d, the better resolution a microscope has. The equation clearly shows that d is highly dependent on the wavelength λ, where short wavelengths are obviously desirable. For normal light microscopy, light in the range of the visible light spectrum (>380 nm) is usually used, resulting in a maximum resolution of around 200 nm. The wavelength of an electron beam is dramatically smaller. **In modern electron microscopy (EM) systems, values around 2 pm are achievable, suggesting a theoretical resolution of ~1 pm. However, the practical resolution with these machines is estimated to be ~0.1 nm due to aberration errors of the electron lenses.** This is still good enough to see individual atoms (Meyer et al. 2008).

Inside these microscopes, an electron beam is generated by the emission of electrons from a glowing cathode. These electrons are subsequently accelerated in a high vacuum by a tunable anode and aligned by a system of electronically charged lenses. **In the field of electron microscopy, two principally different major technologies are known: transmission EM (TEM) and scanning EM (SEM)** (Koning and Koster 2009).

In TEM, the ray of electrons is shone through an extremely thin sample of interest (Fig. 8.2a). Upon interaction with the atoms in the sample, the electrons are scattered and/or absorbed. A detection device behind the sample is then able to generate a magnified image of the modified electron beam that can be observed on a screen or with a camera. TEM thus generates highly resolved images of thin sections of samples. In contrast, SEM uses an electron beam that is scanned over the surface of a fully intact 3D specimen and releases secondary electrons from its surface. These are measured by a detector and generate one pixel of a digital image. By scanning over the surface of the sample very detailed 3D images of surfaces can be obtained (Fig. 8.2b). We have used this approach to document the details of phagocyte contacts to *A. fumigatus* spores (Behnsen et al. 2007a) as well as the fine structures of DNA NETs with

these fungal elements (Bruns et al. 2010). Others have used SEM and TEM to document the uptake of *Aspergillus* spores by alveolar macrophages (Ibrahim-Granet et al. 2003).

Although TEM images give an extremely good resolution of cellular structures, they are typically only 2D. A fairly recent addition to the technology now allows the generation of 3D reconstructions from TEM images without the need for serial sections. This technique is called **electron tomography (ET)**. Here, the thin sample is placed on a rotating device and a series of TEM images from different angles is taken, which then allows reconstruction of the 3D network of observed structures with unprecedented detail (Koning and Koster 2009). This technology has already been used to study the ultrastructure of fungal elements (Hohmann-Marriott et al. 2006). It would be extremely interesting to also use ET for the study of host–pathogen interactions.

Thus, while the advantage of EM obviously lies in its extreme resolving power, the downside is its inability to image live specimens. Furthermore, EM requires extensive sample preparation and a lot of experience both in the use of the microscopes as well as in interpretation of the data. Nevertheless, without doubt the electron microscope has opened to human eyes the fascinating ultrastructural world, which has always intrigued scientists and laymen and will continue to do so in the future. The inability of EM to image live specimens is partly overcome, albeit not with the same resolving power, with new methods in optical microscopy (see next section).

D. Super-Resolution Light Microscopy

For more than 100 years the obtainable maximum resolution of optical microscopes was accepted to be ~200 nm, based on Abbés rules of diffraction (Hell 2009) (see also the previous section on electron microscopy). However, since the 1990s a number of innovative advances have been made that allow resolutions of up to ten times higher using currently available commercial light microscopy systems. Here, we will discuss three key developments in the field: stimulated emission depletion, structured illumination microscopy, and localization microscopy. Unfortunately, not much use has been made of these developments in experimental mycology so far. For a fine review of the use of these novel systems in the general microbiology field the reader is referred to (Coltharp and Xiao 2012). Future work should thus aim at exploiting these techniques for investigating fungal infections and the interaction of fungi with the vertebrate immune system in unprecedented detail.

STED (stimulated emission depletion): STED is principally an advanced method of CLSM. However, rather than using just one blue exciting laser spot, the dimensions of which are limited to the 200 nm size defined by Abbé optics, **STED projects a second, red-colored, doughnut shaped depletion beam over the exciting beam**. This depletion beam has a hole in the middle, where no laser light is emitted. All fluorescence hit by the depletion laser is immediately quenched again due to a process called stimulated depletion. The key feature of STED is that the hole in the center of the doughnut can be adjusted to be significantly smaller than 200 nm, based on the power and the optical shaping of the laser. Thus, the combination of excitation spot and depletion doughnut allows the generation of a much smaller spot of residual excitation than could be obtained with a focused excitation laser alone (Eggeling et al. 2009). **This small spot of residual excitation increases the optical resolution in the *x*,*y*-plane by a factor of four to eight.** In modern commercial systems, this is indeed achieved by the click of a mouse on the control software. The advantage in resolution is bought at the expense of the very bright light of the depletion beam. Thus, STED imaging is prone to rapid bleaching and phototoxicity, although novel developments such as gated STED reduce this problem (Vicidomini et al. 2011). Furthermore, not all dyes are suitable for STED imaging and there is only the possibility to simultaneously image two colors as opposed to other multicolor options. Finally, STED only increases the resolution in the *x*,*y*-plane, while resolution in the *z*-direction is not changed.

SIM (structured illumination microscopy): SIM uses the projection of a known grating structure into the imaging plane that is recorded together with the emitted fluorescence. By interference with the emitted fluorescence, so-called moiré fringes are generated. These contain additional structural information about the sample that cannot be simply extracted by optical resolution but needs complex mathematical operations (Fourier transformations) to obtain an image. As a result, **SIM increases the resolution in all three directions of space by a factor of at least two** (Schermelleh et al. 2008; Gustafsson 2005). Thus, although not as good as STED, the principal advantage of SIM is the fact that it works with any fluorescent dye and does not use high intensities of light. Thus, it can also be used for long-term time-lapse imaging (Fiolka et al. 2012).

Localization microscopy (PALM/STORM): These approaches exploit the ability of fluorescent dyes to emit light only for short amounts of time, whereby two adjacent molecules rarely emit simultaneously. However, this is typically not seen because conventional fluorescent images are an integrated fluorescence signal of many molecules permanently illuminated over a long time. But, when a given field of fluorescent molecules is excited with stroboscopic light rather than continuous illumination, at one stroboscopic pulse only a fraction of molecules will fluoresce. When the next stroboscopic pulse hits the system, a separate fraction of molecules will glow. If, by this approach, a large series (typically several thousand images) of stroboscopic images is taken, for statistical reasons all available fluorescent molecules will have glowed at least once. The important feature is that by this approach two directly adjacent molecules will not shine on the same frame of the series, but only on separate frames. This fact allows their **optical separation as two molecules, rather than as one larger fluorescent entity**. The image generated by this method is not a classical picture like that made by a PMT. Instead, from each light spot detected in the series of images the exact center of the generating fluorescent spot will be calculated from fitting the Gaussian light distribution with nanometer precision. This calculated molecular position will be artificially set as the position of a positive pixel whose superimposition with all other found spot positions generates the final super-resolution image. As a result, **localization images have a "pointillist" appearance but their resolution (or rather, their precision in exactly localizing the source of a fluorescence signal) in the *x*,*y*-plane can reach values of 20 nm or better** (Coltharp and Xiao 2012; Hell 2007). To generate this extreme resolution, PALM/STORM requires very specific dyes and experimental conditions (such as stringent buffer conditions on fixed samples). This renders the technology rather complicated and limited in its use. Nevertheless, commercial systems are available and if the requests by researchers rise, it is expected that suppliers will respond with developments towards greater ease of use.

E. Flow Cytometry

A very powerful approach for analyzing host–fungal interactions is flow cytometry. Here, rather than imaging a few cells or fungal elements with very high resolution, many cells (typically many thousands) are imaged in a short time with only limited resolution. Flow cytometry uses a constant flow of liquid droplets to enclose individual cells or cell pairs. These cell-containing droplets subsequently cross one or more laser beams. By hitting intra-and extracellular structures, the laser light is diffracted and scattered light is produced. Light that is diffracted on the surface of the spherical particles is then detected by a spectral detector in a 180° angle relative to the excitation beam (forward scatter, FSC). The diffraction angle allows the calculation of the cell size so that this detector (i) counts all cells that pass the detection optics and (ii) assesses their individual relative size. A second detector is located (side scatter, SSC) at a 90° angle. The amount of light detected here directly correlates with the amount of intracellular structures (granules) of a cell or cell–cell pair.

In addition, cells can be labeled with a variety of fluorescent agents that bind to their surface or intracellularly. If, for example, a fluorescently labeled monoclonal antibody is used

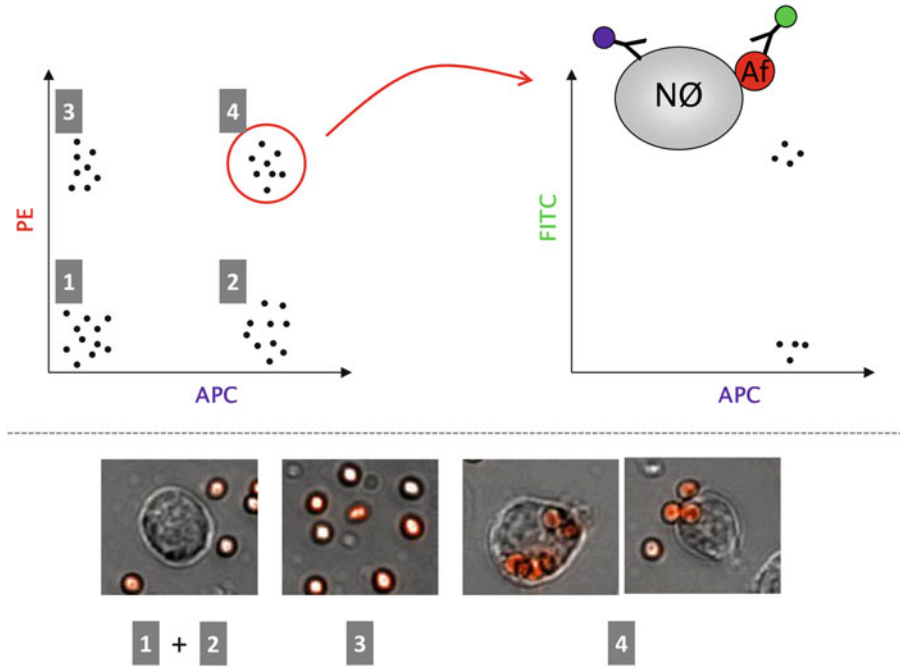

Fig. 8.3. Quantification of phagocytic events by flow cytometry. Example of how phagocytic events can be analyzed by a flow cytometric approach. The background of this experiment were mice that had been infected intratracheally with genetically modified fungal spores, expressing the red fluorescent protein tdTomato. After an incubation time of several hours, the immunological infiltrate was washed out of the lung by a bronchoalveolar lavage followed by monoclonal antibody staining specific for neutrophil granulocytes (clone 1A8 coupled to the fluorescent dye allophycocyanine, APC). After flow cytometric analysis, four clearly distinguishable cell populations are visible by plotting the APC fluorescence versus the tdTomato signal detected in the PE channel (see *left* part of Fig. 8.1): Population *1* constitutes cells that are not neutrophils and that are not co-localized with any fungal spores. Cell population *2* consists of neutrophils that are also not in contact with the fungal particles. The majority of population *3* is most likely composed of free fungal spores but also other (immune) cells that are in contact with the spores are found here. Cell population *4* is the group of interest, where many neutrophils are found that have internalized at least one or more spores. These cells are double-positive for both APC as well as the tdTomato signal. However, especially for neutrophils, it is well known that these cells, besides phagocytosing fungal morphotypes, also attach these entities to their surface, thereby collecting a large number of them. This complex is of course also double-positive for both types of fluorescence and hence generates a potential source of error for this quantitative approach. One way to eliminate false positive events is to add a second antibody (labeled with the green fluorophore fluorescein isothiocyanate, FITC) specific for the fungal spores (AF). Neutrophils (Nϕ) that have spores attached to their surface are then additionally stained green so that these events can be excluded from the analysis. Please note that the image only shows theoretical flow cytometry data for reasons of simplicity. Real dot plots contain many hundreds to thousands of dots

that can bind to a specific surface structure of a cell, this cell type can be selectively labeled in a heterogeneous cell suspension (Fig. 8.3). **By running many thousands of cells through the flow cytometer and counting all labeled cells, the relative number of these cells in a mixture can be easily obtained.** Introduced as principal technology in 1969 (Hulett et al. 1969), flow cytometry has revolutionized many scientific fields, especially immunology. Importantly, **in addition to imaging cells, flow cytometry can also be used to physically sort them according to predetermined parameters of scatter and fluorescence** (fluorescence activated cell sorting, FACS). There are many applications in the field of antifungal immunology that can benefit from the technique, e.g., measuring the genomic response of sorted epithelial cells after

phagocytosis of *Aspergillus* spores (Gomez et al. 2010) or quantifying the organ-specific immune response after invasive candidiasis (Lionakis et al. 2011), the response of mast cells towards the fungal cell wall component zymosan (Yang and Marshall 2009), or the uptake and killing of conidia by diverse phagocytyes (Jhingran et al. 2012).

In general, any approach that allows the fluorescent labeling of fungal elements and immune cells separately, in vitro, within true infection models, or even from patient samples, is able to be analyzed on a large scale by flow cytometry.

A critical limitation of flow cytometry is that it is not able to show individual events directly. Instead they are transformed into dot plots or histograms as output graphs. But, if for example, phagocytosis is the investigated process, flow cytometry is hardly able to distinguish whether co-associated fungal elements and immune cells are only attached to each other's surfaces or whether a phagocyte has entirely internalized the pathogen. A novel invention called **imaging flow cytometry** has changed this. Here, in principle, the same hardware setup as inside a flow cytometer is used. However, rather than just recording the total fluorescence of an event passing the laser beams, it is photographed by a fast, multicolor camera (Barteneva et al. 2012). At first glance the resulting data look like conventional flow cytometry plots but they allow **a detailed look at each single dot of a dot plot as a photographic image**. Here, phagocytosis can easily be distinguished from simple attachment. This technology has been used to show that treatment of mice with the drug sulfasalazine during pulmonary pneumocystosis enhances fungal uptake by alveolar macrophages and leads to more rapid clearing of the fungal infection (Wang et al. 2010). Thus flow cytometry, with its ability to rapidly scan and/or sort cells in large numbers, and imaging flow cytometry are two very potent imaging technologies, both in experimental as well as clinical mycology.

However, although important observations can be made in a reduced environmental complexity in vitro, one has to keep in mind that an in vitro situation never fully represents the in vivo environment of a living organism. Therefore, it is always important to think about experimental approaches that allow the in vivo observation of the investigated phenomena. This is more complicated to establish and often limited in its application possibilities but the results obtained from intravital imaging experiments deliver more meaningful results. In fact, due to the increasing availability of in vivo imaging techniques, observations made purely in vitro are nowadays often considered as potentially suffering from artifact. As a result, researchers wishing to publish work on dynamic cellular processes today are often asked to verify their in vitro data in an in vivo setup. To help find the right approach and judge the feasibility of a reviewer's comment, we will now discuss different systems that can generate intravital imaging data.

F. Intravital 2-Photon Microscopy

The principal construction of an intravital 2-photon (2-P) microscope is similar to the CLSM, as discussed above. Thus, a laser beam is scanned over the sample and the generated fluorescence is detected by PMTs and reconstructed into a full multicolor picture (Niesner et al. 2008a; Niesner et al. 2007). However, the difference lies in the use of the laser and the physics behind the generation of the fluorescent signal. For the generation of fluorescence, a fluorophore needs to absorb an incoming photon that has the correct wavelength so that the delocalized electrons of the fluorophore can be lifted from a ground state to an excited state. Upon return to the ground state, the electrons emit a fluorescence photon that is slightly redshifted in relation to the exciting photon. Hence, the color of fluorescence is slightly redder than the color of excitation. Typical fluorophores need excitation wavelengths in the visible spectrum. However, the principal problem of visible light photons is that they cannot penetrate very deeply into thick tissue due to massive diffraction. As a result, intravital microscopy with visible light using a conventional CLSM is possible, but does not reach large depths in tissue (Gunzer et al. 2004; Stoll et al. 2002). Importantly, wavelengths between 800 and 1,200 nm (near infrared) have excellent

tissue penetration capabilities and thus would be perfect for imaging in vivo (Konig 2000). However, conventional fluorophores cannot be excited by these photons because they possess too little energy.

This is where the 2-photon process comes into play. If laser radiation of near-infrared color is very intense, one fluorophore can be hit at almost the same time by two or more of these red photons. Then, they combine their energy on the surface of the fluorophore and excite it to emit normal fluorescence. At the same time, this allows the use of the red laser wavelengths that give good tissue penetration. The enormous intensity of laser light required for 2-PM is generated by the use of pulsed rather than continuous wave lasers (as in conventional CLSM). Pulsed lasers (typically titanium–sapphire solid-state lasers) have immense amounts of photons in extremely short-lived pulses (10^{-13} s pulse duration). When these are highly focused by the optics of the 2-PM system, the energy at the focal spot is high enough to allow the 2-P process to occur at a meaningful frequency that enables imaging (Germain et al. 2006). At the same time, the system is inherently confocal as no out-of-focus fluorescence is generated because the extreme level of photon flux required for the excitation of fluorescence is only reached at the center of the focal spot of the optics.

2-PM is the most widely used technology for high-resolution intravital imaging in experimental animals and we have made extensive use of the technology to investigate antifungal immunity (Hasenberg et al. 2011c; Nitschke et al. 2008; Bruns et al. 2010). But, 2-PM offers more than just the ability to image fluorescent structures deep inside scattering tissue. One powerful approach is **fluorescence lifetime imaging (FLIM)**. For FLIM, not only the intensity of fluorescence as such, but also its decay characteristics after a single excitation are measured. This can be nicely employed to study the characteristics of endogenous fluorescent molecules such as NAD(P)H. This important coenzyme has a characteristic 2-P excitation at 760 nm and an emission peak at around 460 nm. Within a cell (e.g. a neutrophil granulocyte), NAD(P)H can exist as the free coenzyme. This has a fluorescence lifetime of ~430 ps. However, there are more than 100 enzymes known that can bind NAD(P)H as a coenzyme, and when bound to a protein the lifetime of NAD(P)H changes quite substantially. We have shown that this feature is able to very specifically detect the NAD(P)H molecules inside of a neutrophil granulocyte because they are bound to NAD(P)H oxidase, the key enzyme for the generation of fungitoxic reactive oxygen species (Niesner et al. 2008b). When bound to the oxidase, the lifetime of NAD(P)H was stretched to 3.6 ns. Spots with this lifetime showed a characteristic enrichment at sites where neutrophils touched fungal elements and could be selectively quenched with the addition of inhibitors of the oxidase (Niesner et al. 2008b). Because there are many more enzymes to which NAD(P)H can bind, it is tempting to speculate that each one shows a characteristic lifetime of the associated NAD(P)H molecule and thus can be identified by FLIM without the need for additional staining. In addition, other endogenous fluorophores (e.g., FAD) exist in cells and are able to be investigated by FLIM. Thus, together with the ability for intravital imaging, 2-PM and FLIM are powerful tools for the investigation of host–fungal interactions in vivo.

G. Whole-Body Imaging

Although being very potent for high-resolution imaging at organ level, 2-PM is also limited in its penetration/detection depth. Depending on the type of tissue, several hundred micrometers can be achieved, but it is not possible to scan through larger organs or even whole intact animals. Thus, it is not possible to use the 2-PM technique for whole-body imaging, e.g., if the position or infectious spread of a fungus is to be monitored inside of an experimental animal. To close this gap, different companies offer so-called whole-body imaging systems for small animal research. The first machines that entered the market used the **detection of bioluminescence signals with very sensitive CCD cameras** as their key function. Bioluminescence makes use of luciferases, which are enzymes

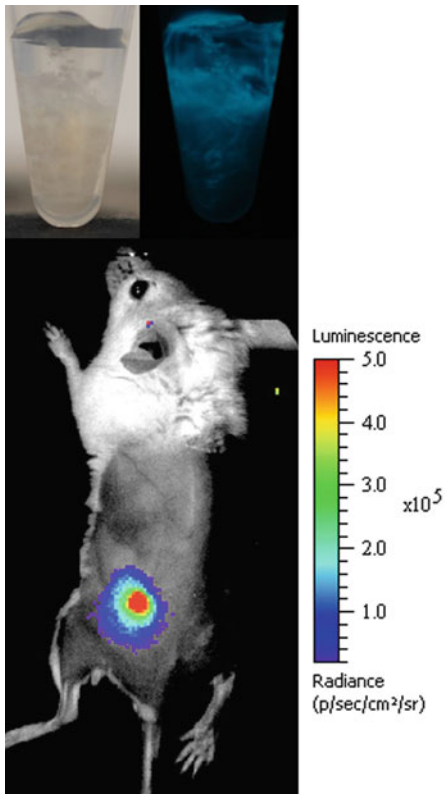

Fig. 8.4. Imaging cutaneous aspergillosis by bioluminescent imaging. In an immunosuppressed mouse infected with 10^4 conidia of a bioluminescent *A. fumigatus* reporter strain that displays the *Gaussia princeps* luciferase on its surface (*top*), localization of the fungal pathogen can be followed in the living animal in a longitudinal fashion. The substrate coelenterazine was applied subcutaneously and emitted photons were detected via a CCD camera to yield a bioluminescence signal that correlates to the fungal burden in the infected tissue (*bottom*)

made by insects, corals, or copepods. By the breakdown of their substrates (e.g., luciferin or coelentaerazine), luciferase is able to generate photons that can be detected with sensitive cameras, even if they are generated deep inside the tissue. The big advantage of this enzyme system lies in the spontaneous release of photons during the chemical reaction without an exciting light source that also would have to pass through the surrounding tissue. Such bioluminescent reporter systems **allow for real-time imaging and longitudinal infection studies, thereby reducing the number of monitored animals and decreasing experimental variability**. However, in contrast to bacterial bioluminescent reporter systems, eukaryotic systems require the addition of an extrinsic substrate. Accordingly, substrate stability, tissue penetration, and uptake by the pathogen are limiting factors for bioluminescence imaging of fungal infections. Based on pioneering studies in the human commensal *Candida albicans* (Doyle et al. 2006; Enjalbert et al. 2009), we have expressed the *Gaussia princeps* copepod luciferase on the surface of *A. fumigatus* to demonstrate that cutaneous aspergillosis is clearly detectable in infected animals (Fig. 8.4) and dependent on the innate immune system for growth control (Donat et al. 2012). Others have shown that pulmonary and systemic infections with *A. fumigatus* can also be monitored by this method when expressing the firefly luciferase from *Photinus pyralis* intracellularly (Brock et al. 2008; Jouvion et al. 2012; Ibrahim-Granet et al. 2010). Meanwhile, such whole-body scanners also make use of the **detection of fluorescence signals**. With the introduction of a variety of red and far-red dyes it became possible to excite these fluorophores from the outside with light of a very long wavelength. This relatively energy-poor light is able to penetrate biological tissue very efficiently, thereby enabling the use of fluorescent probes for this application. Bioluminescent fungal strains interacting in vivo with fluorescently labeled immune cells may therefore provide a deeper understanding of the intimate host–pathogen interplay during infection.

III. Clinical Imaging

Imaging fungal infections is not only a decisive tool for academic research but it is also a central technology for modern clinical routine in wards treating patients at risk of infection. Thus, it is important to consider the available options that help clinicians to clearly identify a fungal infection and, more importantly, to distinguish it from other situations that might cause inflammatory states in patients.

The main arms of clinical imaging are **ultrasound**, **X-ray** (conventional and **computed tomography,** CT), magnetic resonance imaging (**MRI**), and contrasting methods using radioisotopes, especially **PET** and scintigraphy. All of these techniques have been used in fungal diagnosis, even though MRI and CT have become the central methods in routine clinical application.

A. Ultrasound

Ultrasound uses sound waves with intensities above 16 KHz that are radiated from a transducer into the body. They are echoed back from reflecting tissues and bodily liquids or gases with different efficiencies, allowing them to be structurally distinguished upon re-detection in the transducer. Gases and bone are very effective echoing structures, whereas blood and other liquids give poor echoes. Thus, blood and other liquids will give black pixels in an ultrasound image while bone and gases give white pixels, thereby allowing the reconstruction of an irradiated tissue with useful resolution. The advantages of ultrasound are that it is fast, generates tissue sectioning images on the fly, and is without ionizing radiation. Thus, ultrasound is considered harmless. The disadvantages are the relatively low resolution and absence of specific contrasting methods, except Doppler sonography for visualizing flow. Collectively, sonography can be used for diagnosis of fungal infections such as in the urinary tract (Kauffman et al. 2011) or the heart (Ronco et al. 2010), but due to the limitations of the technology ultrasound has not found entry into routine application.

B. X-Ray and Computed Tomography

X-ray uses highly intense photons of wavelengths between 10^{-8} and 10^{-12} m. They can cross bones and tissues easily at full thickness, and upon traveling through different structures are more or less efficiently absorbed. After transfer through the body they hit a detection device (photosensitive plates or CCD cameras in modern digital X-ray systems). Structures with high absorptive potential (especially bones) will give white pixels (because only a few X-ray photons can cross the bone and blacken the photosensitive device), whereas soft tissue typically gives gray to black pixels. A conventional X-ray image is a 2D projection of the 3D tissues crossed by the X-ray beam during its journey through the body. This does not give information on the position of structures in space. Therefore, the more advanced method of CT was developed. Here, a patient is analyzed by X-rays that come from different directions in space to generate a depth-encoded section through the body. For a full CT section, X-rays are projected to from a complete 360° circle around the patient and then step-wise along the body length axis to generate a series of sections. Images are no longer directly generated by a detection device but instead need extensive computing efforts to generate precisely located volume-pixels (voxels). The advantage over conventional X-ray is the much better soft-tissue contrast and the 3D information of the investigated organ.

The disadvantage of X-ray in general and of CT in particular is that they use ionizing radiation and thus constitute a carcinogenic potential. Nevertheless, **the easy tissue penetration and excellent contrasting capabilities have made X-ray and CT the most used methods for the diagnosis of fungal infections, especially in the case of invasive aspergillosis** (Brown et al. 2012). However, despite their frequent use, the specific diagnosis of a fungal infection using X-ray or CT is very difficult and prone to error. Typically, radiologists search for a so-called **halo sign** (HS) or **reverse halo sign** (RHS) (Georgiadou et al. 2011; Marchiori et al. 2012) in the lung of patients with suspected fungal infection. These are optical features within a CT image with a central bright area surrounded by a ring of "ground glass opacity" (HS) or the reverse version of these optical features (RHS). Histopathologically, the ground glass structure represents hemorrhage of the lung tissue, while the bright area corresponds to necrosis of the infected lung tissue (Georgiadou et al. 2011). The problem with this approach is twofold: first, as can

be deduced from the description of the HS/RHS, its unequivocal identification is not easy and requires the inspection of CT images by a well-trained expert with a lot of experience in this field. Second, and maybe even more important, HS and RHS are by no means specific for invasive aspergillosis or a fungal infection in general. Instead, since their publication, identical signatures have been found in CT images associated with bacterial or parasitic infections but also in neoplastic disease or systemic disorders such as Wegener's granulomatosis or sarcoidosis (Georgiadou et al. 2011). Thus, **despite their superb optical contrast in human tissue, neither X-ray nor CT are 100% robust tools for the clinical diagnosis of fungal infections**. Yet, next to MRI (see below) they are the best available imaging technology for this purpose to date and will therefore continue to be used until their replacement by better approaches.

C. Magnetic Resonance Imaging

From its physical background, magnetic resonance imaging (MRI) is a very complicated method, the detailed description of which is far beyond the scope of this article. The interested reader is referred to some excellent reviews on the subject (Moonen et al. 1990; Friston 2009). In short, the technology uses extremely strong external magnetic fields to orient the spin axes of atoms, especially hydrogen atoms, in the body of the patient along the orientation of the magnetic field lines. Then, an additional radio frequency electrical field is induced for a short time, which causes a deflection of the spin axis of the nuclei. The rotation of the nuclei with a deflected spin axis around the general orientation of the external magnetic field (precession) induces an electrical signal whose decay with time can be measured (T2 value). In addition, the spin axis slowly returns to its orientation along the outer magnetic field lines and the precession is lost (relaxation time, T1 value). The relaxation time can also be measured. Importantly, the signal strength and the time to full relaxation is dependent on the environment of the atom and thus allows the extraction of information on the surroundings of where the atoms are measured. Using complicated mathematics, the different measured relaxation times and signal intensities allow a picture of the different surroundings of hydrogen atoms within the body to be drawn. Fat tissue, for example, is very bright, whereas the air-filled lung is almost black. It is possible to enhance the contrast, e.g. of blood vessels, by the application of contrasting agents such as gadolinium or gadolinium-labeled particles.

The general advantage of MRI is the lack of ionizing radiation and thus the method has much lower to absent inherent toxicity as compared to X-ray, CT, or imaging based on radionuclides (see below). In addition, **MRI provides an excellent soft tissue contrast** whereby, e.g., a kidney can be reconstructed with the individual nephrons clearly visible whereas CT images show a kidney without much internal structure. The downside of MRI is the enormous technical effort, meaning that only specialized centers can mount the necessary resources. **MRI is equally potent in detecting pulmonary fungal infections as CT. Ideally, both methods can be combined to provide a more robust diagnosis** (Muller et al. 2002). **The significant power of MRI comes with the diagnosis of cerebral fungal infections** (Mullins 2011) where, depending on the measurement used (T1 or T2 weighted), a significant contrast can be obtained that completely circumscribes the fungal lesion inside the brain (Gabelmann et al. 2007; Brown et al. 2012). Nevertheless, **MRI does not allow the specific identification of a fungal infection based on exactly defined parameters**. Instead, like CT, it requires the eyes of very experienced radiology experts and the diagnosis "fungal infection" is based on their interpretation of the imaging data rather than on a non-disputable independent parameter.

D. Positron Emission Tomography

PET uses the ability of some radionuclides to generate and emit positrons, the antiparticles of electrons. When positrons hit an electron in the vicinity, the two particles are annihilated,

which results in the generation of two gamma quanta that each possess the characteristic energy of 511 keV and are emitted at exactly a 180° angle from their origin of generation. The PET detector is able to measure these gamma quanta and also their relative arrival time at the two opposite positions on a ring-shaped collection of detectors around a patient. By correlating these events, it is possible to reconstruct the exact position of the radionuclide inside of the patient's body, from where the positron originated.

The power of the approach is the ability to locate anything associated with the radionuclide inside of a patient. Thus, **by designing tracer molecules that have the ability to localize at clinically important sites inside of a patient and loading these tracers with PET-suitable radionuclides, it is possible to exactly position the radionuclides at this site and therefore to clearly diagnose the presence of this structure inside of the patient.** A typical example used extensively in oncology is FDG. Glucose enriches at sites of heavy cellular metabolism, which are particularly frequent in fast growing tumors. Thus, a patient suffering from a metastasized tumor will enrich FDG both in the primary tumor and also in the metastases, allowing their localization via PET. This principle has led to the widespread use of FDG-PET in oncology (Jones and Price 2012). Despite its success in that field, PET imaging has not been used extensively so far in infection diagnosis and less so in fungal diagnosis (Walker et al. 2007), although it is being discussed (Limper et al. 2011). Interestingly, infection can also compromise oncological PET imaging because a compound such as FDG is not able to distinguish increased metabolic activity due to cancer growth or due to locally enriched immune cells fighting an infectious focus (Sandherr et al. 2001).

Thus, currently there is no tool available in the clinic that allows the specific labeling of fungal elements in a patient's body with a PET tracer and so allow the unequivocal detection of the infection. However, experimental approaches have demonstrated the principal ability of PET to specifically detect fungal infections using a ^{68}Ga-labeled siderophore (Petrik et al. 2012; 2010). Other approaches make use of the intrinsic ability of immune cells to localize places of fungal infection in the body (Bruns et al. 2010) by loading leukocytes with PET tracers and applying them as infection-specific agents. However, the success of this approach has been limited and it has not found widespread application in the clinical routine (Gardet et al. 2010; Dumarey et al. 2006). Other approaches use the radiolabeling of anti-granulocyte antibodies to locate infections in humans, which also sounds promising but is not widely used (Graute et al. 2010). All these approaches would, however, also experience analogous limitations in terms of specificity compared to FDG-PET.

Despite having the ability for highly specific labeling of infectious foci inside of a patient with optimized tracers, PET suffers from limitations in resolution. This is why **modern PET always comes as a combined modality such as PET/CT or, more recently, PET/MRI** (Pichler et al. 2008; Judenhofer et al. 2008). Here, the superb resolution of imaging with CT or MRI is combined with the molecular information yielded from PET. This has proven successful in a clinical study, which also showed the ability of FDG-PET to follow up on the therapeutic success of antifungal therapy (Hot et al. 2011). Thus, **in principle, PET in combination with a high-resolution imaging modality has enormous power to be used as a specific imaging approach for the rapid, non-invasive and definitive diagnosis of fungal infections.**

Next to these obvious advantages, PET suffers from a number of technical drawbacks. First, it uses radioactive tracers that have the intrinsic capability to induce cancer. Next, the need to handle potentially short-lived radioisotopes requires their production on site in expensive cyclotrons. Finally, it requires extensive experience in a clinical center with nuclear medicine and in the management of patients under these regimes. Thus, in the near future any such applications will only be possible in large dedicated centers. Nevertheless, the potential of the technology should continue to be harvested by driving the development of novel molecular tracers that can specifically identify fungal elements throughout the

Table 8.1. Comparison of imaging technologies discussed in this chapter

	Experimental imaging									Clinical imaging				
	Widefield microscopy	CLSM	Electron microscopy	STED	SIM	Localization microscopy	Flow cytometry	Intravital 2-PM	Whole-body imaging	Ultrasound	X-ray and CT	MRI	PET	Combined PET/MRI
Purchase considerations														
Purchase Costs	●●●	●●	●●	●●	●●	●●	●●	●●	●●●	●●●	●	●	●	●
Running Costs	●●●	●●	●●	●●	●●	●●	●●	●●	●●●	●●●	●	●	●	●
System size	●●●	●●	●●	●●	●●	●●	●●●	●●	●●●	●●●	●	●	●	●
Requirements on Installation Site	●●●	●●	●●●	●●	●●	●●	●●●	●●	●●●	●●●	●	●	●	●
Application considerations														
Ease of use	●●●	●●●	●●	●●	●●●	●●	●●	●●	●●●	●●	●	●	●	●
Intravital Application	●	●●	n.a.	●	n.a.	n.a.	n.a.	●●	●●●	●●●	●●●	●●●	●●●	●●●
Flexibility regarding animal type	●●	●●	n.a.	●●	n.a.	n.a.	n.a.	●●	●●	●●●	●●●	●●●	●●●	●●●
In vitro application	●●●	●●●	●●●	●●●	●●●	●●●	●●●	●●●	●●●	n.a.	n.a.	n.a.	●	n.a.
Live cell Observation	●●●	●●	n.a.	●●	●●	n.a.	●●●	●●	n.a.	n.a.	n.a.	n.a.	n.a.	n.a.
3D information	●	●●●	●●	●●●	●●●	●	●	●●●	●	●●	n.a./ ●●●	●●●	●	●●●
Biomarker Detection (sensitivity)	●●	●●	●	●●	●●	●●	●●●	●●	●	●	n.a.	●	●●	●●
Parameter considerations														
Optical resolution	●●	●●	●●●+	●●●	●●	●●●	●	●●	●	●	●	●●	●	●●
3D sectioning	●	●●●	●●	●●●	●●●	●	●	●●	●	●●	n.a./ ●●●	●●●	●	●●●
Time resolution	●●●	●●	n.a.	●●	●●	n.a.	●●●	●●	●●	●●●	n.a./●●	●●	●	●
Data size	●●	●●	●●	●●	●●	●●	●●●	●●	●●●	●●●	●	●	●	●

n.a. non-applicable, ● poor, ●● good, ●●● optimal, + indicates even better

patient's body. A particularly well-suited tool for this would be monoclonal antibodies, which have already shown their potential for the specific detection of fungal infections in experimental systems. Monoclonal antibodies would not only allow the unequivocal diagnosis of the disease using PET but would also be able to highly selectively deliver aggressive ionizing radiation to the fungus as a treatment (Bryan et al. 2012).

IV. Summary and Outlook

In summary, we have given a general overview of existing imaging technologies that can be used efficiently to show fungal pathogens alone or during their interaction with the host immune system (see Table 8.1). The approaches have been used widely in experimental systems and clinically. Future work should exploit the capabilities of novel high-resolution imaging regimes in studying host–fungal interaction in experimental systems. Also, improvements in whole-body intravital microscopy to give better tissue penetration and resolution are highly desirable. **Clinical imaging currently suffers from a dearth in specific tools that allow the unequivocal identification of a fungal infection. Thus, research in this field should aim at developing useful novel molecular tracers.** With a number of exciting concepts at hand, some of which we have briefly mentioned here, we expect a bright future ahead of us for the imaging of fungal infections, both in experimental and clinical systems. Novel developments will then hopefully not only quench our academic thirst but also help patients suffering from life-threatening infections to obtain fast and specific treatment.

References

Barteneva NS, Fasler-Kan E, Vorobjev IA (2012) Imaging flow cytometry: coping with heterogeneity in biological systems. J Histochem Cytochem 60:723–733

Behnsen J, Narang P, Hasenberg M, Gunzer F, Bilitewski U, Klippel N, Rohde M, Brock M, Brakhage AA, Gunzer M (2007) Environmental dimensionality controls the interaction of phagocytes with the pathogenic fungi *Aspergillus fumigatus* and *Candida albicans*. PLoS Pathog 3:e13

Brock M, Jouvion G, Droin-Bergere S, Dussurget O, Nicola MA, Ibrahim-Granet O (2008) Bioluminescent Aspergillus fumigatus, a new tool for drug efficiency testing and in vivo monitoring of invasive aspergillosis. Appl Environ Microbiol 74:7023–7035

Brown GD, Denning DW, Gow NA, Levitz SM, Netea MG, White TC (2012) Hidden killers: human fungal infections. Sci Transl Med 4:165rv13

Bruns S, Kniemeyer O, Hasenberg M, Aimanianda V, Nietzsche S, Thywißen A, Jeron A, Latge JP, Brakhage AA, Gunzer M (2010) Production of extracellular traps against *Aspergillus fumigatus in vitro* and in infected lung tissue is dependent on invading neutrophils and influenced by Hydrophobin RodA. PLoS Pathog 6:e1000873

Bryan RA, Guimaraes AJ, Hopcraft S, Jiang Z, Bonilla K, Morgenstern A, Bruchertseifer F, Del PM, Torosantucci A, Cassone A, Nosanchuk JD, Casadevall A, Dadachova E (2012) Toward developing a universal treatment for fungal disease using radioimmunotherapy targeting common fungal antigens. Mycopathologia 173:463–471

Coltharp C, Xiao J (2012) Superresolution microscopy for microbiology. Cell Microbiol 14:1808–1818

Denning DW, Hope WW (2010) Therapy for fungal diseases: opportunities and priorities. Trends Microbiol 18:195–204

Donat S, Hasenberg M, Schafer T, Ohlsen K, Gunzer M, Einsele H, Löffler J, Beilhack A, Krappmann S (2012) Surface display of Gaussia princeps luciferase allows sensitive fungal pathogen detection during cutaneous aspergillosis. Virulence 3:51–61

Doyle TC, Nawotka KA, Kawahara CB, Francis KP, Contag PR (2006) Visualizing fungal infections in living mice using bioluminescent pathogenic Candida albicans strains transformed with the firefly luciferase gene. Microb Pathog 40:82–90

Dumarey N, Egrise D, Blocklet D, Stallenberg B, Remmelink M, Den MV, Van Simaeys G, Jacobs F, Goldman S (2006) Imaging infection with 18F-FDG-labeled leukocyte PET/CT: initial experience in 21 patients. J Nucl Med 47:625–632

Eggeling C, Ringemann C, Medda R, Schwarzmann G, Sandhoff K, Polyakova S, Belov VN, Hein B, von Middendorff C, Schonle A, Hell SW (2009) Direct observation of the nanoscale dynamics of membrane lipids in a living cell. Nature 457:1159–1162

Enjalbert B, Rachini A, Vediyappan G, Pietrella D, Spaccapelo R, Vecchiarelli A, Brown AJ, d'Enfert C (2009) A multifunctional, synthetic Gaussia princeps luciferase reporter for live imaging of Candida albicans infections. Infect Immun 77:4847–4858

Fiolka R, Shao L, Rego EH, Davidson MW, Gustafsson MG (2012) Time-lapse two-color 3D imaging of live cells with doubled resolution using structured illumination. Proc Natl Acad Sci USA 109:5311–5315

Freifeld AG, Bow EJ, Sepkowitz KA, Boeckh MJ, Ito JI, Mullen CA, Raad II, Rolston KV, Young JA, Wingard JR, Infectious Diseases Society of America (2011) Clinical practice guideline for the use of antimicrobial agents in neutropenic patients with cancer: 2010 update by the Infectious Diseases Society of America. Clin Infect Dis 52:427–431

Friston KJ (2009) Modalities, modes, and models in functional neuroimaging. Science 326:399–403

Gabelmann A, Klein S, Kern W, Kruger S, Brambs HJ, Rieber-Brambs A, Pauls S (2007) Relevant imaging findings of cerebral aspergillosis on MRI: a retrospective case-based study in immunocompromised patients. Eur J Neurol 14:548–555

Gardet E, Addas R, Monteil J, Le GA (2010) Comparison of detection of F-18 fluorodeoxyglucose positron emission tomography and 99mTc-hexamethylpropylene amine oxime labelled leukocyte scintigraphy for an aortic graft infection. Interact Cardiovasc Thorac Surg 10:142–143

Georgiadou SP, Sipsas NV, Marom EM, Kontoyiannis DP (2011) The diagnostic value of halo and reversed halo signs for invasive mold infections in compromised hosts. Clin Infect Dis 52:1144–1155

Germain RN, Miller MJ, Dustin ML, Nussenzweig MC (2006) Dynamic imaging of the immune system: progress, pitfalls and promise. Nat Rev Immunol 6:497–507

Gomez P, Hackett TL, Moore MM, Knight DA, Tebbutt SJ (2010) Functional genomics of human bronchial epithelial cells directly interacting with conidia of Aspergillus fumigatus. BMC Genomics 11:358

Graute V, Feist M, Lehner S, Haug A, Muller PE, Bartenstein P, Hacker M (2010) Detection of low-grade prosthetic joint infections using 99mTc-antigranulocyte SPECT/CT: initial clinical results. Eur J Nucl Med Mol Imaging 37:1751–1759

Gunzer M, Weishaupt C, Hillmer A, Basoglu Y, Friedl P, Dittmar KE, Kolanus W, Varga G, Grabbe S (2004) A spectrum of biophysical interaction modes between T cells and different antigen presenting cells during priming in 3-D collagen and in vivo. Blood 104:2801–2809

Gustafsson MG (2005) Nonlinear structured-illumination microscopy: wide-field fluorescence imaging with theoretically unlimited resolution. Proc Natl Acad Sci USA 102:13081–13086

Hasenberg M, Behnsen J, Krappmann S, Brakhage A, Gunzer M (2011a) Phagocyte responses towards Aspergillus fumigatus. Int J Med Microbiol 301:436–444

Hasenberg M, Köhler A, Bonifatius S, Borucki K, Riek-Burchardt M, Achilles J, Männ L, Baumgart K, Schraven B, Gunzer M (2011b) Rapid immunomagnetic negative enrichment of neutrophil granulocytes from murine bone marrow for functional studies in vitro and in vivo. PLoS One 6:e17314

Hasenberg M, Köhler A, Bonifatius S, Jeron A, Gunzer M (2011c) Direct observation of phagocytosis and NET-formation by neutrophils in infected lungs using 2-photon microscopy. J Vis Exp 52:e2659. doi:10.3791/2659

Hasenberg M, Stegemann-Koniszewski S, Gunzer M (2013) Cellular immune reactions in the lung. Immunol Rev 251:189–214

Hell SW (2007) Far-field optical nanoscopy. Science 316:1153–1158

Hell SW (2009) Microscopy and its focal switch. Nat Methods 6:24–32

Hohmann-Marriott MF, Uchida M, van de Meene AM, Garret M, Hjelm BE, Kokoori S, Roberson RW (2006) Application of electron tomography to fungal ultrastructure studies. New Phytol 172:208–220

Hot A, Maunoury C, Poiree S, Lanternier F, Viard JP, Loulergue P, Coignard H, Bougnoux ME, Suarez F, Rubio MT, Mahlaoui N, Dupont B, Lecuit M, Faraggi M, Lortholary O (2011) Diagnostic contribution of positron emission tomography with [18 F] fluorodeoxyglucose for invasive fungal infections. Clin Microbiol Infect 17:409–417

Hulett HR, Bonner WA, Barrett J, Herzenberg LA (1969) Cell sorting: automated separation of mammalian cells as a function of intracellular fluorescence. Science 166:747–749

Ibrahim-Granet O, Philippe B, Boleti H, Boisvieux-Ulrich E, Grenet D, Stern M, Latge JP (2003) Phagocytosis and intracellular fate of *Aspergillus fumigatus* conidia in alveolar macrophages. Infect Immun 71:891–903

Ibrahim-Granet O, Jouvion G, Hohl TM, Droin-Bergere S, Philippart F, Kim OY, Adib-Conquy M, Schwendener R, Cavaillon JM, Brock M (2010) In vivo bioluminescence imaging and histopathopathologic analysis reveal distinct roles for resident and recruited immune effector cells in defense against invasive aspergillosis. BMC Microbiol 10:105

Jhingran A, Mar KB, Kumasaka DK, Knoblaugh SE, Ngo LY, Segal BH, Iwakura Y, Lowell CA, Hamerman JA, Lin X, Hohl TM (2012) Tracing conidial fate and measuring host cell antifungal activity using a reporter of microbial viability in the lung. Cell Rep 2:1762–1773

Jones T, Price P (2012) Development and experimental medicine applications of PET in oncology: a historical perspective. Lancet Oncol 13:e116–e125

Jouvion G, Brock M, Droin-Bergere S, Ibrahim-Granet O (2012) Duality of liver and kidney lesions after systemic infection of immunosuppressed and immunocompetent mice with Aspergillus fumigatus. Virulence 3:43–50

Judenhofer MS, Wehrl HF, Newport DF, Catana C, Siegel SB, Becker M, Thielscher A, Kneilling M, Lichy MP, Eichner M, Klingel K, Reischl G, Widmaier S, Rocken M, Nutt RE, Machulla HJ, Uludag K, Cherry SR, Claussen CD, Pichler BJ (2008) Simultaneous PET-MRI: a new approach for functional and morphological imaging. Nat Med 14:459–465

Kauffman CA, Fisher JF, Sobel JD, Newman CA (2011) Candida urinary tract infections–diagnosis. Clin Infect Dis 52(Suppl 6):S452–S456

Konig K (2000) Multiphoton microscopy in life sciences. J Microsc 200(Pt 2):83–104

Koning RI, Koster AJ (2009) Cryo-electron tomography in biology and medicine. Ann Anat 191:427–445

Latge JP (1999) *Aspergillus fumigatus* and aspergillosis. Clin Microbiol Rev 12:310–350

Limper AH, Knox KS, Sarosi GA, Ampel NM, Bennett JE, Catanzaro A, Davies SF, Dismukes WE, Hage CA, Marr KA, Mody CH, Perfect JR, Stevens DA (2011) An official American thoracic society statement: treatment of fungal infections in adult pulmonary and critical care patients. Am J Respir Crit Care Med 183:96–128

Lionakis MS, Lim JK, Lee CC, Murphy PM (2011) Organ-specific innate immune responses in a mouse model of invasive candidiasis. J Innate Immun 3:180–199

Marchiori E, Zanetti G, Hochhegger B, Irion KL, Carvalho AC, Godoy MC (2012) Reversed halo sign on computed tomography: state-of-the-art review. Lung 190:389–394

Mech F, Thywissen A, Guthke R, Brakhage AA, Figge MT (2011) Automated image analysis of the host-pathogen interaction between phagocytes and Aspergillus fumigatus. PLoS One 6:e19591

Meyer JC, Girit CO, Crommie MF, Zettl A (2008) Imaging and dynamics of light atoms and molecules on graphene. Nature 454:319–322

Michelio PA (1729) Nova plantarum genera iuxta tournefortii methodum disposita. Bernardo Paperini, Florence

Moonen CT, van Zijl PC, Frank JA, Le BD, Becker ED (1990) Functional magnetic resonance imaging in medicine and physiology. Science 250:53–61

Muller FM, Trusen A, Weig M (2002) Clinical manifestations and diagnosis of invasive aspergillosis in immunocompromised children. Eur J Pediatr 161:563–574

Mullins ME (2011) Emergent neuroimaging of intracranial infection/inflammation. Radiol Clin North Am 49:47–62

Niesner RA, Andresen V, Neumann J, Spiecker H, Gunzer M (2007) The power of single- and multibeam 2-photon microscopy for high-resolution and high-speed deep tissue and intravital imaging. Biophys J 93:2519–2529

Niesner RA, Andresen V, Gunzer M (2008a) Intravital 2-photon microscopy – focus on speed and time resolved imaging modalities. Immunol Rev 221:7–25

Niesner RA, Narang P, Spiecker H, Andresen V, Gericke KH, Gunzer M (2008b) Selective detection of NADPH oxidase in polymorphonuclear cells by means of NAD(P)H-based fluorescence lifetime imaging. J Biophys 2008: 602639

Nitschke C, Garin A, Kosco-Vilbois M, Gunzer M (2008) 3-D and 4-D imaging of immune cells in vitro and in vivo. Histochem Cell Biol 130:1053–1062

Peleg AY, Hogan DA, Mylonakis E (2010) Medically important bacterial-fungal interactions. Nat Rev Microbiol 8:340–349

Petrik M, Haas H, Dobrozemsky G, Lass-Flörl C, Helbok A, Blatzer M, Dietrich H, Decristoforo C (2010) 68 Ga-siderophores for PET imaging of invasive pulmonary aspergillosis: proof of principle. J Nucl Med 51:639–645

Petrik M, Franssen GM, Haas H, Laverman P, Hortnagl C, Schrettl M, Helbok A, Lass-Flörl C, Decristoforo C (2012) Preclinical evaluation of two (68)Ga-siderophores as potential radiopharmaceuticals for Aspergillus fumigatus infection imaging. Eur J Nucl Med Mol Imaging 39:1175–1183

Pichler BJ, Judenhofer MS, Pfannenberg C (2008) Multimodal imaging approaches: PET/CT and PET/MRI. Handb Exp Pharmacol 185:109–132

Romani L (2011) Immunity to fungal infections. Nat Rev Immunol 11:275–288

Ronco F, Simsir S, Czer L, Luo H, Siegel RJ (2010) Incidental finding by two-dimensional echocardiography of a mycotic pseudoaneurysm of the ascending aorta after orthotopic heart transplantation. J Am Soc Echocardiogr 23:580–583

Sandherr M, von Schilling C, Link T, Stock K, von Bubnoff N, Peschel C, Avril N (2001) Pitfalls in imaging Hodgkin's disease with computed tomography and positron emission tomography using fluorine-18-fluorodeoxyglucose. Ann Oncol 12:719–722

Sasse C, Hasenberg M, Weyler M, Gunzer M, Morschhäuser J (2013) White-opaque switching of Candida albicans allows immune evasion in an environment-dependent fashion. Eukaryotic Cell, 12(1):50–58

Schermelleh L, Carlton PM, Haase S, Shao L, Winoto L, Kner P, Burke B, Cardoso MC, Agard DA, Gustafsson MG, Leonhardt H, Sedat JW (2008) Subdiffraction multicolor imaging of the nuclear periphery with 3D structured illumination microscopy. Science 320:1332–1336

Schmidt A (1998) Gerog Fresenius and the species Aspergillus fumigatus. Mycoses 41(Suppl 2):89–91

Seshadri N, Kaur B, Balan K (2007) Disseminated cryptococcosis: detection by F-18 FDG PET. Clin Nucl Med 32:476–478

Shrikanthan S, Aydin A, Dhurairaj T, Alavi A, Zhuang H (2005) Intense esophageal FDG activity caused by Candida infection obscured the concurrent primary esophageal cancer on PET imaging. Clin Nucl Med 30:695–697

Steinberg G (2007) Hyphal growth: a tale of motors, lipids, and the Spitzenkorper. Eukaryot Cell 6:351–360

Stoll S, Delon J, Brotz TM, Germain RN (2002) Dynamic imaging of T cell-dendritic cell interactions in lymph nodes. Science 296:1873–1876

Vicidomini G, Moneron G, Han KY, Westphal V, Ta H, Reuss M, Engelhardt J, Eggeling C, Hell SW (2011) Sharper low-power STED nanoscopy by time gating. Nat Methods 8:571–573

Waibler Z, Sender LY, Merten C, Hartig R, Kliche S, Gunzer M, Reichardt P, Kalinke U, Schraven B (2008) Signaling signatures and functional

properties of anti-human CD28 superagonistic antibodies. PLoS One 3:e1708

Walker RC, Jones-Jackson LB, Martin W, Habibian MR, Delbeke D (2007) New imaging tools for the diagnosis of infection. Future Microbiol 2:527–554

Wang J, Gigliotti F, Bhagwat SP, George TC, Wright TW (2010) Immune modulation with sulfasalazine attenuates immunopathogenesis but enhances macrophage-mediated fungal clearance during Pneumocystis pneumonia. PLoS Pathog 6: e1001058

Yang Z, Marshall JS (2009) Zymosan treatment of mouse mast cells enhances dectin-1 expression and induces dectin-1-dependent reactive oxygen species (ROS) generation. Immunobiology 214:321–330